Optics Letters

Extending the coverage of user-diversified IM-DD PON by FDM: a mathematical model with experimental verification

Peiji Song,[1,2] Yuan Liu,[2] Zhouyi Hu,[3] Chun-kit Chan,[2] and Di Che[1,*]

[1]Nokia Bell Labs, Murray Hill, New Jersey 07974, USA
[2]Department of Information Engineering, The Chinese University of Hong Kong, Shatin, N. T., Hong Kong SAR, China
[3]Department of Electrical Engineering, Eindhoven University of Technology, 5600 MB Eindhoven, The Netherlands
*di.che@nokia-bell-labs.com

Received 29 November 2023; revised 2 April 2024; accepted 3 April 2024; posted 3 April 2024; published 30 April 2024

Future passive optical networks (PONs) call for more flexibility to support diversified users with various rate demands and link qualities. Using traditional time-division multiplexing (TDM), the concept of a flexible rate PON was proposed to accommodate more users with link diversity by rate adaptation. In this Letter, we reveal the PON coverage can be further extended through frequency-division multiplexing (FDM) in the presence of multiuser diversity, namely, (i) there exist users with frequency-dependent link conditions and (ii) the link conditions exhibit disparity among users. We build a mathematical model and propose an optimization algorithm based on the binary tree search to optimize diversity gain. We experimentally verify its feasibility by studying the diversity gain concerning chromatic dispersion, optical path loss, and signal-to-noise ratio (SNR) variation in a 200G-class intensity-modulation direct-detection (IM-DD) system.

https://doi.org/10.1364/OL.514370

With the standardization of next-generation 25G (25GS-PON MSA and IEEE 802.3ca) and 50G (IEEE 802.3ca and ITU-T G.9804.3) passive optical networks (PONs) [1,2], active research efforts have been made for the next-generation PON with a speed of 100G and beyond [3–8]. Coherent detection has been considered a promising candidate, but the shift to coherent techniques means a complete redesign of the architecture for PON, which has been sticking to the simple IM-DD since its birth. Considering single-wavelength 100G/200G intensity-modulation direct-detection (IM-DD) transceivers have become mature in data center applications [9–11], it is possible to develop future 100G or even higher speed PONs based on IM-DD, leveraging the data center components at low cost.

Without resorting to the coherent technique, an IM-DD PON faces some challenges when going for a higher speed, including optical path loss (OPL), chromatic dispersion (CD), and larger user disparity when extending the network coverage [4,7]. While the OPL can be compensated by high-power optical transmitters and receiver-side pre-amplification methods, the latter two potentially limit the network coverage [7]. Traditionally, the specifications of a PON (such as power budget and CD tolerance) are limited by the worst user because the same modulation format and bitrate are served to all users regardless of their actual link conditions. The concept of a flexible rate PON (FLCS-PON) [4] based on time-division multiplexing (TDM) was recently proposed to accommodate user diversity by providing rate adaptation based on each user's link condition. Such rate adaptation is realized by variable-order of the modulation (like NRZ and PAM4), multi-rate forward error correction (FEC) codes, and probabilistic constellation shaping (PCS), which has been shown to greatly improve the aggregated data rate with respect to the traditional fixed-rate PON in a user-diversified network. While the original FLCS-PON proposal is based on single-carrier PAM formats, it can be extended by multicarrier formats such as discrete-multi-tone (DMT) and multi-band carrierless amplitude and phase (MB-CAP) modulations [3,5,6], which achieve a more flexible rate adaptation by adjusting the modulation format per subcarrier. These multicarrier schemes are still compatible with TDM, where each user occupies the entire spectrum during a time slot. To distinguish different formats in TDM systems, we put the modulation format after the term "TDM" in this Letter (e.g., TDM-PAM and TDM-DMT).

Multicarrier modulations can also be utilized for frequency-division-multiplexed (FDM)-PON [12,13]. In this case, each user no longer occupies the entire spectrum but is assigned a portion of the frequency band. Distinguished from previous multicarrier PON demonstrations, a recent proposal [14,15] reveals that it is possible to achieve an FDM diversity gain by optimizing the subcarrier assignment to the end users with disparity (i.e., different link conditions). The diversity gain is potentially achievable when both conditions are met: (i) there exist users with frequency-dependent link conditions, and (ii) the link conditions exhibit disparity among users. Intuitively speaking, a poor user in the FDM system gets a chance to choose among its available subcarrier set to avoid bad subcarriers, and hence suffers less from its poor link condition (in contrast, a TDM user is forced to use the entire spectrum). In other words, if a PON consists of some good users, it can potentially accommodate poor users by FDM, which effectively extends the network coverage. Moreover, FDM can exploit entropy loading (EL), a proven capacity-approaching technique in bandwidth-limited

systems with colored signal-to-noise ratio (SNR) [16,17]. Unfortunately, the previous works [14,15] only provide an empirical algorithm for subcarrier assignment with no mathematic model to support the diversity gain in a theoretical manner and is not guaranteed to find the optimum subcarrier assignment under arbitrary user diversity.

In this Letter, we abstract the subcarrier assignment task in a user-diversified FDM-PON as an optimization model and propose a generic algorithm to maximize the diversity gain in IM-DD PONs with colored SNRs and user disparity. The proposed method is compatible with any multicarrier format like MB-CAP and DMT, and we use DMT as a proof-of-concept example. It is worth noting that we compare the optimized FDM scheme with TDM-DMT rather than the conventional TDM-PAM in this Letter, because the comparison between PAM and DMT is a complex topic depending on the power constraint in the transmitter (see Ref. [17] for details). Briefly speaking, in a channel with a colored SNR profile, DMT is commonly regarded as advantageous over PAM to accommodate the frequency-resolved SNR through adaptive loading per subcarrier basis [17]; on the other hand, PAM may exhibit an optical modulation amplitude (OMA) gain over DMT due to its lower peak-to-average power ratio (PAPR). Considering such a discussion is more related to the modulation formats in a point-to-point system and is not relevant to the multiuser diversity gain, we exclude it from the scope of this Letter. We choose TDM-DMT as the comparison baseline for a fair claim of the diversity gain achieved by FDM-DMT. We experimentally verified the feasibility of our scheme by studying the gain with disparities on CD, OPL, and SNR variation in a 200G-class IM-DD system.

We first intuitively explain the basic concept of achieving the FDM diversity gain by optimizing subcarrier assignment. In the toy example of Fig. 1, we show the achievable information rate (AIR) per subcarrier for two users sharing the same bandwidth resource with six subcarriers. Without loss of generality, we assume the two users target the same rate. Using TDM, the AIR per user is 74.1 Gb/s calculated by the harmonic average. For FDM, the six subcarriers will be assigned to the two users, and Fig. 1 presents a pair of opposite strategies: (i) better subcarriers are assigned to the better user, and (ii) better subcarriers are assigned to the worse user. The latter achieves an AIR of 81 Gb/s, larger than the AIR of TDM, while the former gets a smaller (68 Gb/s) AIR. This indicates that the capacity of FDM is highly affected by way of subcarrier assignment, and a proper assignment enables a diversity gain over TDM. The algorithm in Ref. [14] follows the latter concept.

We now elucidate our optimization model. Considering the downstream in PON with U users, we use a probe signal with N subcarriers to obtain the channel conditions of all users. The estimated AIR of the j-th subcarrier on the i-th user is denoted as r_{ij}, and the entire matrix $[r_{ij}]$ fully characterizes the user diversity. The matrix $[x_{ij}]$ is used to denote the subcarrier assignment, and we set $x_{ij}=1$ if the j-th subcarrier is assigned to the i-th user; otherwise, $x_{ij}=0$. Therefore, the AIR of the i-th user is $G_i=\sum_{j=1}^{N} r_{ij}x_{ij}$, and the total AIR of all U users is $I=\sum_{i=1}^{U}\sum_{j=1}^{N} r_{ij}x_{ij}$. Besides, x_{ij} must satisfy the constraint that $\sum_{i=1}^{U} x_{ij}=1$, for $j=1, \ldots, N$, as each subcarrier is assigned to one user. The optimization problem can be summarized as the following integer linear programming (LP) problem:

$$\begin{aligned} &\underset{[x_{ij}]}{Maximize}\ I=\sum\nolimits_{i=1}^{U}\sum\nolimits_{j=1}^{N} r_{ij}x_{ij},\\ &Subject\ to\ \sum\nolimits_{i=1}^{U} x_{ij}=1,\ j=1,\ \ldots,\ N;\\ &\qquad (w_i-\alpha)G_1 \le G_i \le (w_i+\alpha)G_1,\ i=2,\ \ldots,\ U;\\ &\qquad x_{ij}\in\{0,\ 1\}, i=1,\ \ldots,\ U, j=1,\ \ldots,\ N, \end{aligned} \tag{1}$$

where the subcarrier assignment matrix $[x_{ij}]$ is what we want to optimize, and w_i is the weight coefficient of i-th user's rate target (G_i) with respect to user 1 (i.e., $G_i=w_iG_1$). To make Eq. (1) more feasible to solve, we introduce an adjustable error factor α to relax the strict constraints $G_i=w_iG_1$. A larger error factor α makes it easier or faster to find the solution at the cost of a larger rate mismatch. In most cases, such theoretical rate mismatch can be accommodated in practice by EL whose fine rate granularity per subcarrier enables the precise AIR match for every user.

The most straightforward method to solve Eq. (1) is the full enumeration algorithm, namely, traversing all the possible combinations of $[x_{ij}]$ with $\{x_{11}, \ldots, x_{UN}\}\in\{0, 1\}^{UN}$ and selecting the combination yielding the maximum objective value. However, the total number of possible combinations exponentially increases with UN as 2^{UN}, resulting in an unacceptable high computational complexity. An LP problem can be simplified by relaxing its constraints. Considering the technique of solving the LP problem with continuous constraints is mature [18, section 4.3], we propose to simplify the enumeration algorithm using binary tree search optimization, whose principle is depicted in Fig. 2. We first relax all the integral constraints $x_{ij}\in\{0, 1\}$ into the continuous constraints $x_{ij}\in[0, 1]$ for $i=1, \ldots, U$ and $j=1, \ldots, N$. The objective value using all continuous constraints is denoted as I_0 in Fig. 2, and it is obvious that I_0 is the largest achievable value of Eq. (1). We iteratively add the integral constraint starting from x_{11}, with the remainder variables being continuous. With $x_{11}\in\{0, 1\}$, we can get two branches with

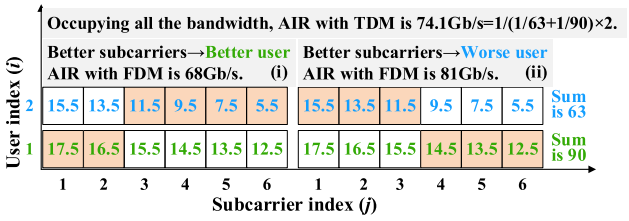

Fig. 1. Example that shows the influence of subcarrier assignment on the aggregated AIR, with two users targeting the same AIR. The numbers inside the boxes refer to the AIR per subcarrier.

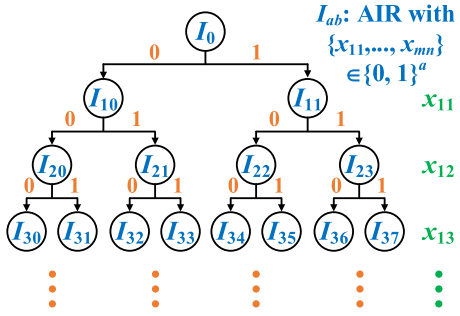

Fig. 2. Simplified algorithm proposed to solve Eq. (1) effectively.

optimum objective values of I_{10}, and I_{11} (I_{10}, $I_{11} \le I_0$), respectively. The integral constraint is then applied to x_{12} that $\{x_{11}, x_{12}\} \in \{0, 1\}^2$, while the remainder variables are still continuous, leading to four branches with the optimum objective values being I_{20}, I_{21}, I_{22}, and I_{23} (I_{20}, $I_{21} \le I_{10}$, and I_{22}, $I_{23} \le I_{11}$), respectively. While repeating the above operations for the following variables, most branches will be terminated early from the following three aspects: (i) as each subcarrier can only be assigned to one user, some branches will automatically terminate starting from certain layers; e.g., in the branch $x_{11} = 1$, the following sub-branches with $x_{i1} = 1$ for $i = 2, \ldots, U$ will end because the 1st subcarrier has already been assigned to user 1; (ii) with the increasing number of integral constraints in Fig. 2, it may lead to no solution of Eq. (1) at some nodes; (iii) if the objective value I_1 at one layer is larger than I_2 at the previous layer, we can stop creating new branches from I_2. For instance, if $I_{20} > I_{11}$, we can stop all the branches from node I_{11}. Finally, we can get the maximum optimum objective value after we set all variables into integral constraints that $\{x_{11}, \ldots, x_{UN}\} \in \{0, 1\}^{UN}$. The corresponding branches lead to the subcarrier assignment matrix $[x_{ij}]$, namely, the solution of the optimization problem. Generally, this branch-and-bound algorithm can reduce the node number from $O(2^{UN})$ to $O(poly(UN))$ [19], where "*poly*" stands for polynomials. Note that in a PON system, the optimal subcarrier assignment will not change frequently because the fiber channels are relatively stable. Therefore, the complexity of the subcarrier assignment algorithm is a secondary consideration in real-world implementations, whose analysis is left for future works.

In an IM-DD PON, the link conditions are mainly diversified in CD and OPL, which represent two types of diversity: (i) a colored (i.e., frequency-dependent) SNR difference produced by CD (ii) a white one (i.e., the same SNR variation for all subcarriers) due to the OPL difference. User diversity has been studied by a variety of literatures by digging into field-deployed PON data [4,20]; e.g., in Ref. [20] that studied Orange's subscribers in France, the dispersive range of the system can be from 0 to 78 ps/nm; meanwhile, the worst case of OPL difference between ONUs may reach up to 20 dB according to the ITU-T PON standard [21]. Besides, the frequency-dependent SNR variations greatly influence the FDM gain. This work aims to study the impact of each factor on the diversity gain individually. Therefore, rather than emulating a real-world PON configuration, we study a series of systems with one variable factor while fixing the others. To facilitate the experimental study of the CD influence, we conduct the experiment at C-band with a maximum CD of 68 ps/nm corresponding to the ~17-km distance at 1342 nm [20]. As a typical example, the maximum OPL difference in the experiment is set to 10 dB.

Figure 3 showsthe IM-DD experimental setup that suffers from a bandwidth limit mainly from the transmitter. The DMT modulation has a DFT size of 2048, a number of effective subcarriers of 1000, and a cyclic prefix length of 16. Without loss of generality, we use the bit error rate (BER) as the loading target, which was combined with a look-up table-based EL [16] to search among the PCS formats with square (16/64/256/1024) QAM templates. We use the generalized mutual information (GMI) under binary hard-decision (HD) decoding (hGMI) as the AIR metric [22]. We use a 1:2 power splitter to emulate two users with an identical rate target. The findings can be easily extended to multiple users.

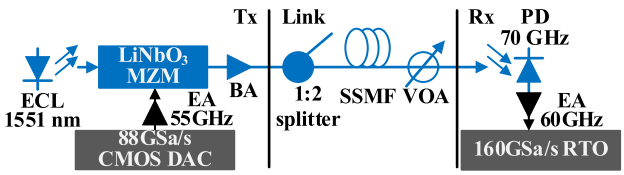

Fig. 3. Experimental setup. ECL, external cavity laser; EA, electrical-amplifier; DAC, D/A converter, MZM, Mach–Zehnder modulator; BA, booster-amplifier; SSMF, standard single-mode fiber; VOA, variable optical attenuator; PD, photodiode; RTO, real-time oscilloscope. The DAC and MZM have a gradually decayed frequency response with analog bandwidth at class 30 GHz.

Figure 4 plots the experimental results, where the BER target is set to be 0.01. For the dispersion case, the SNR curves with varying CDs are plotted in Fig. 4(a2). The frequency-selective fading becomes severer as CD increases, leading to a monotonically decreasing AIR, as shown by the orange curve in Fig. 4(a1). Since the TDM rate is limited by the worst channel, it also monotonically reduces. In comparison, the FDM rate almost remains unchanged. This is because the fading happens at high frequencies, which is almost transparent to poor users who are assigned low-frequency subcarriers, as shown by the subcarrier assignments in Fig. 4(a3). This clearly indicates how FDM extends the network coverage. The maximum FDM gain exceeds 15% given the CD difference of 68 ps/nm, as presented by the blue curve in Fig. 4(a1). For the case with OPL disparity, Fig. 4(b2) depicts the SNR curves with several OPLs. Due to the decreased SNR, both the AIRs of FDM and TDM decrease with the increase of OPL, but FDM maintains its gain over TDM, and the gain increases with a larger OPL difference, as shown in Fig. 4(b1). The maximum gain is close to 25% around a 10-dB OPL difference. Taking this maximum gain as an example, Fig. 4(b3) shows the effect of the error factor α on the number of combinations required by the branch-and-bound algorithm. It can be seen that the branch-and-bound algorithm significantly reduces the number of enumeration method $2^{2\times 1000}$, and slightly increasing α helps reduce the number of combinations. It is worth mentioning that the α-induced rate mismatch can be fully accommodated using the fine-granularity EL. Hence, the error factor α in practical applications can be slightly larger to save running time ($\alpha = 0.03$ in this work).

We also study the influence of the frequency-dependent SNR variation on the diversity gain, where CD and OPL were fixed at 0 ps/nm and 0 dB, respectively. We use pre-equalization to emulate different degrees of SNR variations. Due to the bandwidth limit of the transmitter in our experiment, the pre-equalization that enhances the high-frequency signal power reduces the SNR variation among the subcarriers. We choose linear pre-equalization in this work, and the term "depth" refers to the power response difference between the highest frequency and DC in the linear pre-equalizer. Figure 4(c2) plots the SNR profiles with various pre-equalization depths, and Fig. 4(c3) shows the frequency response of the pre-equalization. Since proper pre-equalization can help improve the system performance, the AIRs of FDM and TDM increase first and then decrease, as plotted in Fig. 4(c1). Despite this, when the increased depth weakens the SNR variation among subcarriers, the diversity gain decreases, as we expected.

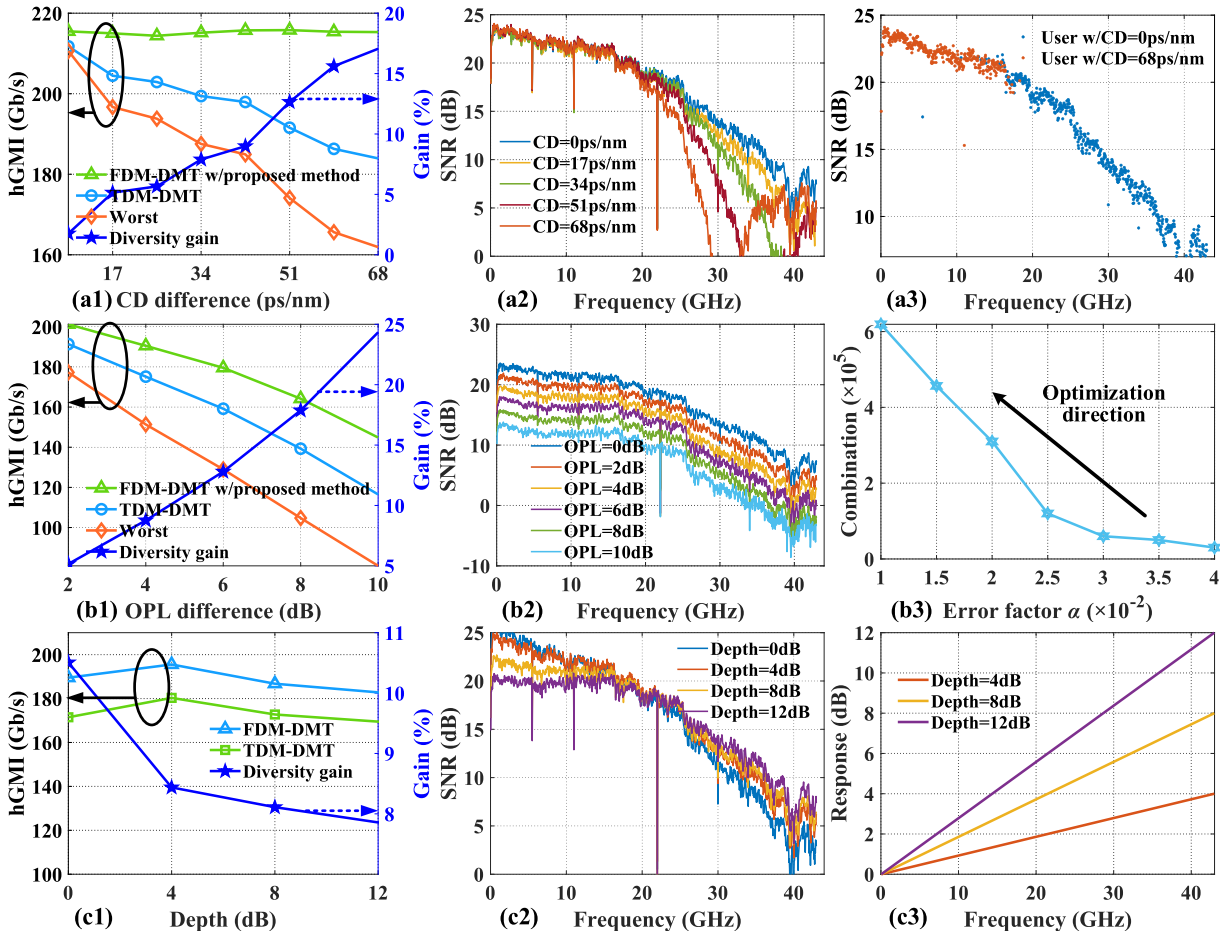

Fig. 4. Diversity gain with respect to the link diversity in (a) CD, (b) OPL, and (c) SNR variation among subcarriers; (a2), (b2), and (c2) are the corresponding SNR curves. (a3) Subcarrier assignment example at the maximum gain of (a1); (b3) optimization of α at the maximum gain of (b1); (c3) pre-equalizer responses. "Worst": all the users operate at the worst condition without rate adaptation.

In conclusion, we build a mathematical model to formalize the subcarrier assignment in FDM-PONs in the presence of arbitrary user diversity as an optimization problem and solve it with a simple branch-and-bound algorithm aiming to maximize the gain of FDM over TDM. This provides theoretical support for the diversity gain and indicates that an FDM-PON may tolerate more poor users when good users exist, effectively extending the coverage of future PONs with larger user disparity.

Disclosures. The authors declare no conflicts of interest.

Data availability. Data underlying the results presented in this paper are not publicly available at this time but may be obtained from the authors upon reasonable request.

REFERENCES

1. "Physical layer specifications and management parameters for 25 Gb/s and 50 Gb/s passive optical networks," IEEE 802.3ca Task Force, http://www.ieee802.org/3/ca/index.shtml.
2. "Optical systems for fiber access networks," ITU-T Q2/SG15, https://www.itu.int/en/ITU-T/studygroups/2017-2020/15/Pages/q2.aspx.
3. V. E. Houtsma and D. T. van Veen, J. Lightwave Technol. **38**, 1 (2020).
4. R. Borkowski, Y. Lefevre, A. Mahadevan, *et al.*, J. Opt. Commun. Netw. **14**, C82 (2022).
5. G. Liu, J. Zhou, Y. Huang, *et al.*, J. Opt. Commun. Netw. **15**, 442 (2023).
6. J. Zhou, J. He, X. Lu, *et al.*, J. Opt. Commun. Netw. **14**, 944 (2022).
7. R. Bonk, E. Harstead, R. Borkowski, *et al.*, J. Opt. Commun. Netw. **15**, 518 (2023).
8. Z. Xing, K. Zhang, X. Chen, *et al.*, in *2023 Optical Fiber Communications Conference and Exhibition (OFC)* (2023), paper Th4C.4.
9. D. Che, Y. Matsui, R. Schatz, *et al.*, in *2021 Optical Fiber Communications Conference and Exhibition (OFC)* (2021), pp. 1–3.
10. S. Yamauchi, K. Adachi, H. Asakura, *et al.*, *2021 Optical Fiber Communications Conference and Exhibition (OFC)* (2021), pp. 1–3.
11. A. Uchiyama, S. Okuda, Y. Hokama, *et al.*, in *Optical Fiber Communication Conference (OFC) 2023, Technical Digest Series* (Optica Publishing Group, 2023), paper M2D.2.
12. D. Qian, N. Cvijetic, J. Hu, *et al.*, IEEE Photonics Technol. Lett. **21**, 1265 (2009).
13. I. N. Cano, X. Escayola, P. C. Schindler, *et al.*, J. Opt. Commun. Netw. **7**, A73 (2015).
14. D. Che and X. Chen, in *49th European Conference on Optical Communications (ECOC)* (2023).
15. D. Che, in *Optical Fiber Communication Conference (OFC)* (2024), paper W1E.3.
16. D. Che and W. Shieh, Opt. Express **27**, 9321 (2019).
17. D. Che and X. Chen, J. Lightwave Technol. **42**, 588 (2024).
18. S. Boyd and L. Vandenberghe, *Convex Optimization* (Cambridge University Press, 2004).
19. D. R. Morrison, S. H. Jacobson, J. J. Sauppe, *et al.*, Discrete Optimization **19**, 79 (2016).
20. G. Simon, F. Saliou, P. Chanclou, *et al.*, in *European Conference on Optical Communications (ECOC)* (2020), paper Tu2J-7.
21. "10-gigabit-capable symmetric passive optical network (XGS-PON)," Recommendation ITU-T G.9807.1 (2016).
22. G. Böcherer, "Achievable rates for probabilistic shaping," arXiv, arXiv:1707.01134 (2017).